Available online at www.sciencedirect.com

ScienceDirect

Procedia Engineering 160 (2016) 191 – 198

Procedia Engineering

www.elsevier.com/locate/procedia

XVIII International Colloquium on Mechanical Fatigue of Metals (ICMFM XVIII)

Pressure, Temperature and Dwell Time Effects on Fatigue Life in 304 Stainless Steel using a R5-based Mechanistic Fatigue Model

T. O. Erinosho*[,a], P. Li[a], C. E. Truman[a] and D.J. Smith[+]

[a]*Solid Mechanics Group, Department of Mechanical Engineering, University of Bristol, BS8 1TR, Bristol, UK*
[+]*Deceased 13th November 2015*

Abstract

This paper aims to evaluate the effects of pressure, temperature, pipe wall thickness and dwell time on fatigue life in 304 stainless steel. For a given dwell time and temperature-internal pressure combination, fatigue life is calculated using the mechanistic fatigue model (MFM) presented. In addition, the influence of pipe wall thickness is also examined. The MFM uses Tresca strain range for initiation and Rankine strain range to account for crack growth rate up to a crack limiting length. The results showed that fatigue life was generally lower for a given load combination in the thinner pipe considered given its smaller surface area compared to the thicker pipe. This led to higher plastic strains and consequently, faster crack growth rates. Also, dwell time influences fatigue life with longer dwell times found to be more damaging. However, the influence of dwell time is tightly coupled with pipe wall thickness as it determines the nature of the thermal gradients developed.

Peer-review under responsibility of the University of Oviedo

Keywords: Fatigue; Dwell; 304 Stainless Steel

1. Introduction

This paper evaluates the fatigue response of a 304 Stainless Steel (SS) pipe subjected to thermo-mechanical loading using a mechanistic fatigue model (MFM). Pipes used in nuclear power plants undergo cycles of heating and cooling. These successive thermal transients cause expansion (due to heating) and contraction (due to cooling), which eventually lead to fatigue crack initiation and propagation under favourable conditions. Assuming the inner

* Corresponding author. Tel.: +44 (0) 117 331 5911.
E-mail address: tomiwa.erinosho@bristol.ac.uk

1877-7058
Peer-review under responsibility of the University of Oviedo
doi:10.1016/j.proeng.2016.08.880

wall of a pipe is heated, heat transfers from the hot to the initially cool outer surface. Depending on the dwell time of the applied heat, the stress distribution across the pipe wall will vary. For example, a long high temperature dwell applied to the pipe's inner wall will lead to expansion and the development of stresses which may cause crack initiation. Assuming the yield stress is attained, plastic strains which promote crack propagation will be developed. Alternatively, a shorter dwell time is more damaging in terms of crack initiation but less so for crack propagation. Further, the thermal gradient developed which causes the pipe to expand unevenly also results in stresses which can promote crack initiation as well as propagation. Therefore, this paper aims to achieve two main goals using a R5-based MFM. First, it illustrates the effects of combined thermo-mechanical loading on fatigue life in 304 SS for a range of dwell times. And second, it evaluates the coupling between pipe wall thickness, dwell and fatigue life.

Numerous models have been developed to predict fatigue life in industrial components. For example, the R5 model [1] was originally developed in 1990 by UK Central Electricity Generating Board (CEGB)/Nuclear Electric but is currently maintained by EDF Energy to cater for life predictions in steels at high temperatures (generally above 500^0C). It is UK nuclear power industry standard, frequently used in safety cases for structural integrity assessments of Advanced Gas-cooled Reactor (AGR) components operating in the creep range. The model accounts for crack initiation and growth due to thermo-mechanical loading and has been revised extensively in the literature e.g. [2]. Other methods such as AEA method [3], Brown and Buckthorpe [4], Modified Crack Growth Model [5] have also been developed. For example, the Modified Crack Growth Model [5] used to predict crack growth below 200μm suggests that crack initiation may be influenced by barriers such as grain boundaries and assumes a non-linear relationship for crack growth rate proposed by Gao et al. [6]. *Stress-based* models such as Sines' criterion [7], *Strain-based* models originating from the Manson-Coffin-Basquin curve established for push pull tests [8, 9] and *Energy-based* models such as Smith-Watson-Topper's criterion [10] have also been developed. The stress and strain based criterions were developed to account for the equivalent strain due to multiaxiality and can be applied flexibly in more established approaches such as AEA or the R5 methods. The energy based models were developed to account for energy dissipation on the basis that crack nucleation which is the precursor to initiation can be adequately captured [11]. However, due to the complexities associated with these models such as material specificity due to texture effects for example, simplistic models such as R5 are prevalent in applied research and is therefore used in this study.

In this paper, a description of the finite element model adopted is presented in Section 2 followed by the MFM in Section 3. Next, a systematic study to evaluate the effects of dwell, pipe wall thickness, pressure and temperature on fatigue life is presented and discussed in Section 4. Finally, conclusions are presented in Section 5.

2. Finite Element Model

The 2-D stepped pipe shown in Figure 1 was modelled in ABAQUS using axisymmetric boundary conditions and temperature dependent material properties summarized in Table 1. The pipe has two sections (A and B) which are 310mm long each. Sections A and B have wall thicknesses of 30.4mm and 15.2mm respectively and each section was modelled in ABAQUS independently as a pipe with uniform wall thickness. An approximate mesh area of 0.5×0.5 mm^2 was adopted and a decoupled thermo-mechanical analysis was undertaken. That is, the pipe is first subjected to cyclic thermal loading and then, the temperature distribution output is assigned as a predefined field for the subsequent mechanical analysis [12]. In the thermal analysis, a heat transfer analysis was prescribed using DCAX4 element type whereas the static mechanical analysis used CAX4R element type. Note that a heat transfer coefficient of 22860W/m^2 [13] was applied and, the material properties in Table 1 were used in the kinematic elastic-plastic analyses. The temperature dependent material properties were obtained from [14] for 304 SS. The yield strength was calculated using expressions by Leax [15] such that

$$Y = 175 - 0.342T + 7.1 \times 10^{-4}T^2 \quad (1)$$

$$H = 24010 - 0.00454T^2 \quad (2)$$

$$\sigma_0 = Y + H\varepsilon_0 \quad (3)$$

where T represents temperature and ε_0 is a reference strain. The yield strength was calculated using Equation (3) by setting the reference strain $\varepsilon_0 = 0$ and the temperature dependent peak stress was obtained at $\varepsilon_0 = 0.01$. This is summarized in Table 1. Note, Poisson ratio is assumed to be 0.31.

3. Fatigue Life Prediction in Stainless Steel

A mechanistic fatigue model (MFM) that accounts for the phases of crack initiation and propagation is used here. This is detailed in Section 3.1 followed by a description of its implementation into MATLAB in Section 3.2. The constants in the model were calibrated and presented in Section 3.3.

3.1. Description of Mechanistic Fatigue Model

The mechanistic fatigue model described here is based on the R5 approach [1]. Under favourable conditions, a crack will initiate at the surface of a specimen and then propagate through the thickness. The crack initiation length (a_i) is assumed as 0.2mm defined in R5 [1]. The crack propagation phase then ranges from $a = 0.2$mm to $a = a_f$ where a_f is the crack length at failure [1]. The number of cycles N_i to initiate a crack with length, a_i , is calculated here using [16]

$$N_i = A(\Delta\varepsilon_T)^b \quad (4)$$

where A and b are material specific constants and, ε_T is the Tresca strain calculated using [17]

$$\varepsilon_T = \frac{1}{(1+\upsilon)}(\varepsilon_3 - \varepsilon_1) \quad (5)$$

where υ is the Poisson ratio and ε_3 and ε_1 are principal strains in the 1- and 2- directions specified in Fig. The next phase of crack growth (N_g) from a_i to a_f is calculated using [16]

$$N_g = \frac{da}{B(a)(\Delta\varepsilon_R^i)^c} \quad (6)$$

where B is a material specific constant, $da = 0.2$ is the integration length, a is the instantaneous crack length and $\Delta\varepsilon_R^i$ is the Rankine strain range at a noting that the Rankine strain is the maximum principal plastic strain. The instantaneous Rankine strain range $\Delta\varepsilon_R^i$ is used to account for strain gradient effects. It is worth highlighting that the Tresca criterion is used for initiation because it accounts for the maximum shear difference whereas the Rankine strain range is used for crack propagation because it is a conservative measure of plastic strain. The mechanistic fatigue model was implemented in MATLAB based on the algorithm presented in the next section.

3.2. Implementation of Mechanistic Fatigue Model in MATLAB

The flowchart in Figure 2 shows the implementation of the MFM in MATLAB. More specifically;

1. Beginning of the routine.
2. The finite element model is built in ABAQUS and elastic-plastic analyses are undertaken using the appropriate material properties, boundary conditions and loading regimes. The calculated strains are used as input to calculate the number of initiation and growth cycles.
3. The number of cycles to initiate a crack is obtained from Equation (4). The Tresca strain range is calculated by evaluating the difference between the peak and minimum mechanical strain given by the Logarithmic Strain minus Thermal strain. The number of cycles obtained using Equation (4) represents a 0.2mm long crack based on the initiation data used for calibration.
4. The number of cycles to grow the crack from the initiation length (a_i=0.2mm) to a crack limiting length is calculated using Equation (6).
5. The number of cycles to grow a 3mm ($N_{f3\text{mm}}$) crack is calculated.
6. End of routine

3.3. Calibrated Fatigue Constants

The constants in Equations (4) and (6) i.e. A, b, B and c are calibrated using experimental S-N fatigue data for 304 SS shown in Figure 3 [18]. Figure 3 is an example of the best fit fatigue life data for 304 SS in air. The number of cycles to initiate a crack approximated using the empirical expression developed in the R5 routine is also shown. The R5 expression is presented in Appendix A. A region of interest is specified in Figure 3 over which the constants in Equations (4) and (6) are calibrated. The region of interest is selected due to the higher confidence in the best fit to experimental data under low cycle fatigue compared to high cycle fatigue. The MFM values in Table 2 were calibrated on the basis that a_f =3mm based on the experimental best fit in Figure 3. The cycles for initiation and total fatigue life calculated using the calibrated MFM values are shown in Figure 3 and a good agreement is observed for all strain ranges considered. On this basis, the number of cycles to grow a fatigue crack to any crack limiting length between 0.2mm and 3mm can be calculated. This is used in the next section to evaluate the influence of pipe thickness, dwell, temperature and pressure on fatigue life in 304 SS.

4. Systematic study of Fatigue using the MFM

The goal of this paper is to use the MFM presented in Section 3 to evaluate the influence of pipe thickness, dwell time, temperature and pressure on fatigue life of the 304 SS stepped pipe shown in Fig. The finite element analyses presented here are first validated in 4.1. Next, the results from a systematic study on the effects of pipe thickness, dwell time, pressure and temperature is presented in 4.2 followed by a discussion in 4.3.

4.1. Validation of Finite Element Analysis (FEA)

In order to validate the FEA presented here, an analysis similar that presented by Gurdal and Xu is undertaken [19]. The inner wall temperature of the 15.2mm pipe wall thickness shown in Fig was ramped from 38^0C to 343^0C in 3 seconds, held at this temperature for 237 seconds, ramped back to 38^0C in 3 seconds and held for a further 237 seconds. The temperature output from the pipe was then adopted as input into a mechanical analysis in order to convert into strains noting an added constant internal pressure of 17.2MPa. Following the analyses, the maximum and minimum mechanical strains are obtained by subtracting the thermal strains (THE) from the logarithmic strain (LE) as summarized in Table 3. The maximum strain is considered as the peak strain during the heating cycle and the minimum is obtained after the thermal shock i.e. upon ramping down from 343^0C to 38^0C over 3 seconds. Note, the results in Table 3 are measured on the inner surface of each pipe. The mechanical strains in this work compare well with that presented by Gurdal and Xu [19] as seen in Table 3. The differences seen are attributed to small variations in material properties adopted in both studies.

4.2. Results

The influence of thermo-mechanical loading on fatigue life is investigated using the MFM presented in Section 3. Two studies are investigated. First, the influence of dwell time on fatigue life is presented and second, the effects of pipe wall thickness are evaluated. It is worth noting that, the term fatigue life here represents the number of cycles to grow a crack to a limiting length of 1mm.

Consider Figure 4a for example, Section A (30.4mm pipe wall thickness) of the pipe in Figure 1 was subjected to varying combinations of thermal loads and constant internal pressure. For the thermal load, the base temperature was constant in all cases i.e. 38^0C. Hence, $\Delta T = 120^0\mathrm{C}$ represents cyclic thermal loading from 38^0C to 158^0C and similarly, $\Delta T = 160^0\mathrm{C}$ represents cyclic thermal loading from 38^0C to 198^0C. For each thermal analysis, the inner wall of the pipe is ramped up from the base temperature (38^0C) to the peak temperature over 3 seconds, it is held at this temperature for the duration of the dwell, ramped back to the base temperature over 3 seconds and then held at this temperature for the specified dwell time. For each thermal load, an associated constant internal pressure is also applied. Subsequently, the mechanical strains are calculated by subtracting the thermal strains from the logarithmic strains and inputted into the MFM in order to calculate the fatigue life (development of a 1mm crack).

The summary of the fatigue life for each thermo-mechanical load combination is presented such as Figures 5 and 6 which represent the 30.4mm and 15.2mm pipe wall thicknesses respectively for the three dwell times considered. In both figures, the temperature change (peak temperature minus base temperature) is shown on the y-axis and the applied internal pressure is shown on the x-axis. The contour lines represent the logarithm of the number of cycles to the limiting crack length for each combination of thermo-mechanical load applied. The results in Figures 5 and 6 are discussed next.

4.3. Discussion

The results in Figures 5 and 6 which represent the fatigue lives of the 30.4mm and 15.2mm thick pipes under a range of thermo-mechanical load combinations are discussed here in terms of two main factors. These are: *dwell time* and *pipe wall thickness*.

Influence of Dwell Time

Three dwell times are considered (137, 237 and 337 seconds). That is, the temperature of the pipe is raised from the base to the peak temperature, held for the duration of the dwell time, ramped back to the base temperature and then held again for the duration of the dwell time at that temperature. Dwell time can significantly affect fatigue life as seen in Figure 6 which compares fatigue life at a given temperature and internal pressure for the three dwell times considered. It is clear from Figure 6a and less pronounced in Figure 6b that longer fatigue life is observed at lower dwell time. It is worth noting that this response is tightly coupled with pipe wall thickness which is discussed later. However, Figure 6a shows that the effect of dwell on fatigue life becomes smaller with increasing dwell time. This implies that the effect of thermal shock following a shorter dwell time is less damaging compared to longer dwell. This is because the pipe thickness is more uniformly heated to a higher temperature for longer dwell leading to more thermal expansion, higher stresses and consequently, higher plastic strains which promotes accelerated crack growth rate.

Influence of wall Thickness

The influence of wall thickness on fatigue life of a pipe subjected to thermo-mechanical loading is discussed here using the two wall thicknesses considered in this study (15.2mm and 30.4mm). First consider Figure 6, it is clear that pipe wall thickness influences its sensitivity to dwell time. In Fig. a, the thicker pipe (30.4mm) showed more pronounced sensitivity to dwell compared to the 15.2mm thick pipe. Now consider Figure 7 which shows the evolution of fatigue life with internal pressure at a constant temperature. It is clear from Figure 7 that more pronounced differences are seen in the 30.4mm pipe wall thickness. This behaviour is also replicated in Figure 8 which shows the evolution of fatigue life with temperature at constant internal pressure. Due to the pipe wall thickness, thermal gradients will exist and this is also coupled with the dwell time. It is worth noting that the heat is applied to the inner wall of the pipe for the duration of the dwell time resulting in heat transfer from the inner to the outer wall which is still at lower temperature.

Consider the 15.2mm pipe wall thickness, a temperature and resulting Rankine strain is developed for 137 seconds dwell case shown in Figure 9a. This distribution changes marginally by increasing the dwell time to 237 seconds and less so by increasing to 337 seconds. This is because thermal steady state has been achieved at 237 seconds therefore, increasing the dwell time will have no effect on changing the temperature distribution across the pipe wall. For this reason, the Rankine strain developed at 337 seconds dwell is similar to 237 seconds. Now, consider a similar distribution in the 30.4mm pipe wall thickness shown in Figure 9b. It is immediately clear that significant differences in Rankine strain exist depending on dwell time. This results from the thermal gradients which develop due to the pipe wall thickness given that thermal steady state has not been achieved. Therefore, a different temperature distribution is developed for each dwell time consequently leading to changes in Rankine strain.

It is worth highlighting the generally lower fatigue lives calculated in the 15.2mm compared with the 30.4 mm pipe wall thickness. By comparing Figure 4 and 6, fatigue life is generally lower in the 15.2mm pipe for the same temperature and internal pressure combination. This is explained using Figure 9 which shows the evolution of Rankine strain range measured from the inner pipe wall. It is clear that the absolute values of Rankine strain are generally larger in the 15.2mm pipe wall thickness compared to 30.4mm. This is attributed to the fact that the 15.2mm pipe is under higher stress at a given load given its smaller surface area compared to the 30.4mm pipe wall thickness. This consequently leads to higher plastic strains and faster crack growth rate.

Comments on the MFM

The popular industrially applied model, R5, was developed to predict fatigue life for high temperature applications (>500^{0}C). The R5 approach appears to be comprehensive enough to broadly account for crack initiation and propagation including effect of multiaxiality which is a significant contributing factor to fatigue life. Initiation in the R5 approach is modelled using an empirical equation (Equation A1 in Appendix A) developed based on striation counting and subsequent deduction of number of growth cycles from total number of applied cycles. However, the model is limited because the testing upon which the R5 was developed was undertaken over a narrow strain range and at 550^0C. Despite the need for a broad range of tests to obtain crack initiation and propagation data in order to fully inform the MFM, the model has shown success as a useful tool to in the study presented here.

5. Conclusions

This paper has evaluated the effects of wall thickness, pressure, temperature and dwell time on fatigue life in 304 SS using the presented MFM. The MFM was used to calculate the number of cycles to grow a crack to a limiting length. The results showed that:

- Fatigue life is generally lower in the thinner pipe considered given its smaller surface area compared to the thicker pipe wall. This leads to higher plastic strains and consequently, faster crack growth rates in the thinner pipe.
- Dwell time influences fatigue life with longer dwell times found to be more damaging.
- The influence of dwell time is tightly coupled with pipe wall thickness as it determines the nature of thermal gradients developed.
- The MFM is a useful tool for predicting fatigue life and for undertaking the systematic studies presented here.

Appendix A. R5 model

The R5 model provides an empirical expression used to approximate the number of cycles for crack initiation (N_i) given the number of cycles to failure (N_f). N_f is obtained from the fatigue life best fit curve for 304 SS in air shown in Fig. . Using this, the initiation cycles N_i are determined from

$$ln(N_i) = ln(N_f) - 8.06N_f^{-0.28} \qquad \text{(A1)}$$

where N_i represents the number of cycles to develop a 0.2mm crack. Note, N_f is assumed to corresponds to a 3mm crack. The constants in Equation (4) which represents initiation were calibrated in the region of interest specified in Figure 1 using the initiation cycles obtained from Equation (A1). Next, the constants in Equation (6) which represents crack growth were subsequently calibrated by accounting for the number of growth cycles between initiation and fatigue life specified by the best fit curve in Figure 3. The calibration routine is such that the error was minimized between combinations of constant for both Equations (4) and (6) in order to obtain accurately calibrated value. It is worth highlighting that strain gradient effects were ignored during calibration of Equation (6). This assumption is valid for thin round bar samples from which the best fit fatigue curve in Figure 3 was obtained. The instantaneous Rankine strain range was later adopted in order to account for strain gradient effects resulting from varying pipe wall thicknesses.

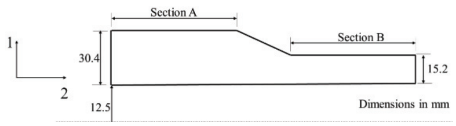

Fig. 1. Schematic of 2-D axisymmetric stepped pipe subjected to thermo-mechanical loading

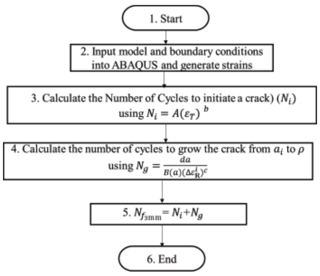

Fig. 2. Flowchart to implement the MFM for initiation and growth prediction up to 3mm in MATLAB

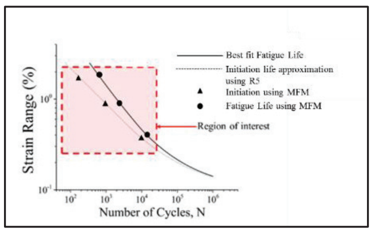

Fig. 3. Experimental Fatigue life of 304 SS in air showing the best fit and number of cycles for crack initiation [20]. The fatigue data in the region of interest is used to calibrate the constants in Equations (4) and (6).

Table 1. Temperature dependent material properties used for the finite element analysis [14].

Temperature (^{0}C)	**Young's Modulus (MPa)**	**Mean Expansion Coefficient (mm/mm/^{0}C)**	**Density (Kg/m^3)**	**Specific Heat (J/Kg.K)**	**Conductivity W/(m^{0}C)**	**Yield Strength ($\varepsilon_0 = 0$), MPa**
20	195000	1.53E-5	8030	473	14.8	168.44
100	189000	1.62E-5	8000	501	16.2	147.9
200	183000	1.70E-5	7960	531	17.9	134
250	179000	1.74E-5	7930	539	18.6	133.87
300	176000	1.77E-5	7910	550	19.4	136.3
350	172000	1.79E-5	7890	557	20.1	142.27

Table 2. Summary of constants used in the MFM to calculate fatigue life.

A	*b*	*B*	*c*
0.006	-2.545	4	1.65

Table 3. Mechanical strains on the inner wall of the stepped pipe obtained by subtracting thermal strain (THE) from the total strain (LE)

Pipe Thickness (mm)	LE11-THE11		LE22-THE22		LE33-THE33		Total Principal Strain Range (%)	
	max	min	max	min	Max	min	This work	Gurdal and Xu [19]
15.2	0.0081	-0.0091	-0.0042	0.0042	-0.0052	0.0062	1.72	1.68

(a) 137 Seconds Dwell Time (b) 237 Seconds Dwell Time (c) 337 Seconds Dwell Time

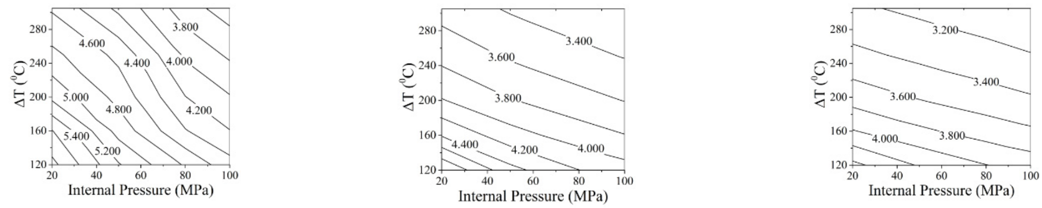

Fig.4. Log of fatigue life for differing combinations of temperature ranges and internal pressure for the three dwell times considered. Note, the fatigue life is calculated using the MFM and represents the number of cycles to grow a 1mm crack in Section A (30.4mm pipe wall thickness) shown in Figure 1.

(a) 137 Seconds Dwell Time (b) 237 Seconds Dwell Time (c) 337 Seconds Dwell Time

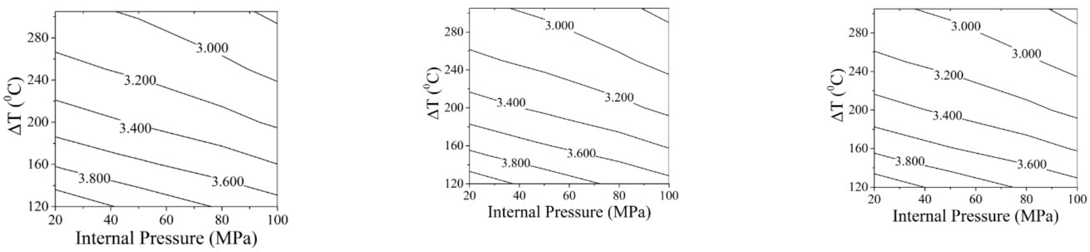

Fig.5. Log of fatigue life for differing combinations of temperature ranges and internal pressure for the three dwell times considered. Note, the fatigue life is calculated using the MFM and represents the number of cycles to grow a 1mm crack in Section B (15.2mm pipe wall thickness) shown in Figure 1.

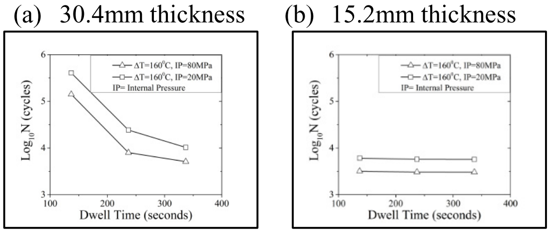

Fig. 6. Evolution of fatigue life with dwell time for the two pipe wall thicknesses considered

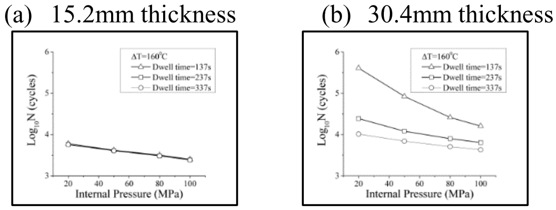

Fig. 7. Evolution of fatigue life with internal pressure at constant temperature for the two pipe wall thicknesses considered

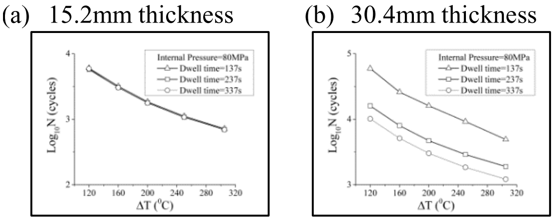

Fig. 8. Evolution of fatigue life with temperature at constant internal pressure for the two pipe wall thicknesses considered

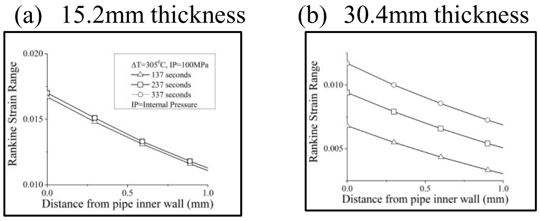

Fig. 9. Evolution of Rankine strain range from the inner surface of the pipe wall for the two pipe wall thicknesses considered

References

[1] R. Hales, Nuclear Electric (1990).
[2] D.M. Knowles, Procedia Engineering 86 (2014) 315-326.
[3] P. C., AEA Technology Internal Report.
[4] M.W. Brown, D. Buckthorpe, SIWG/LASG/P(84)198 (1984).
[5] R.P. Skelton, Materials at High Temperatures 32 (2015) 323-339.
[6] N. Gao, M.W. Brown, K.J. Miller, Fatigue & Fracture of Engineering Materials & Structures 18 (1995) 1407-1421.
[7] I.V. Papadopoulos, P. Davoli, C. Gorla, M. Filippini, A. Bernasconi, International Journal of Fatigue 19 (1997) 219-235.
[8] L.F. Coffin, Current Contents/Engineering Technology & Applied Sciences (1982) 22-22.
[9] S.S. Manson, G.R. Halford, J.J. Blass, S.Y. Zamriki, Journal of Engineering Materials and Technology-Transactions of the Asme 99 (1977) 283-286.
[10] K.N. Smith, P. Watson, T.H. Topper, Journal of Materials 5 (1970) 767-&.
[11] V.V.C. Wan, D.W. MacLachlan, F.P.E. Dunne, International Journal of Fatigue 68 (2014) 90-102.
[12] G. Wu, D.J. Smith, D. Tanner, Proceedings of the ASME 2015 Pressure Vessels & Piping Division Conference PVP2015-45235 (2015).
[13] R.R. PLC, Internal Report EDNS9701653958 (2015).
[14] ASME, II Part D (Metric) Materials (2010).
[15] T.R. Leax, Bettis Atomic Power Laboratory.
[16] G. Wu, D. Smith, D. Tanner, Proceedings of the ASME 2015 Pressure Vessels & Piping Division Conference (2015).
[17] U.S. Fernando, M.W. brown, K.J. miller, Third international conference on Biaxial/Multiaxial fatigue (1989).
[18] O.K. Chopra, D.J. Gavenda, Journal of Pressure Vessel Technology-Transactions of the Asme 120 (1998) 116-121.
[19] R. Gurdal, S. Xu, Proceedings of the ASME 2008 Pressure Vessels & Piping Division Conference (2008).
[20] O.K. Chopra, Argonne National Laboratory Internal Report (2002).